Laser power-meter comparison at far-infrared wavelengths and terahertz frequencies

2012 Metrologia 49 583

(http://iopscience.iop.org/0026-1394/49/4/583)

Metrologia **49** (2012) 583–587 doi:10.1088/0026-1394/49/4/583

Laser power-meter comparison at far-infrared wavelengths and terahertz frequencies

John Lehman[1], Marla Dowell[1], Nina Basta Popovic[2], Kerry Betz[3] and Erich Grossman[1]

[1] National Institute of Standards and Technology, Boulder, CO 80305, USA
[2] Department of Electrical and Computer Engineering, McGill University, Quebec, Canada H3A 0G4
[3] Department of Mathematics, California Institute of Technology, Pasadena, CA 91125, USA

E-mail: lehman@boulder.nist.gov

Received 2 April 2012, in final form 1 June 2012
Published 5 July 2012
Online at stacks.iop.org/Met/49/583

Abstract
We have evaluated the responsivity of seven different thermal detectors compared to an electrically calibrated photoacoustic reference detector at 119 µm (2.5 THz) and 394 µm (0.76 THz) laser wavelengths. Among the thermal detectors is an electrically calibrated thermopile having a vertically aligned carbon nanotube array as the absorber. We document the uncertainty contributions attributable to the photoacoustic reference detector along with a definition of a calibration factor based on the measurement protocol. The expanded relative uncertainty ($k = 2$) and a calibration factor of each detector are tabulated.

(Some figures may appear in colour only in the online journal)

1. Introduction

Instrumentation for measuring laser power at terahertz (THz) frequencies and far-infrared (FIR) wavelengths is important for new and existing technologies for a variety of applications [1]. In this range of the electromagnetic spectrum we are, however, at the frontier of our calibration services at NIST, in this case as millimetre-wave and terahertz applications (free-space propagation) progress to higher frequencies and infrared applications progress to longer wavelengths. One could make the case for a source-based rather than a detector-based calibration, but that is beyond the scope of this paper [2]. This investigation is limited to a measurement of detector responsivity, traceable to SI units by electrical calibration. The method of electrical substitution is the basis of all laser power-meter calibrations (ranging from 157 nm to 10.6 µm) at NIST.

At NIST and elsewhere the development of suitable sources and detectors for FIR laser power meters is being established. Steiger and co-workers demonstrated a detector-based calibration with traceability to a cryogenic radiometer [3]. In the past we have reported a thermopile detector having a vertically aligned carbon nanotube array (VANTA) as the absorber for the FIR [4]. In this work, we summarize the evaluation of this VANTA thermopile detector along with several detectors that are commercially available at wavelengths of 119 µm (2.5 THz) and 394 µm (0.76 THz).

2. Measurement description

The measurement method is direct substitution with an electrically calibrated reference detector. The measurement included a total of eight detectors: two pyroelectric detectors, five thermopile detectors and one photoacoustic detector as the calibrated reference. One pyroelectric detector and the photoacoustic detector each had a chromium-metal absorber (the detector's electrode). Each of the other detectors had some sort of carbon-based black coating. All detectors were obtained from commercial sources with the exception of the NIST VANTA thermopile detector. The reference detector used for these measurements was produced by Thomas Keating[4] (the reference detector is also referred to as the 'TK meter'). To our knowledge, there is no other description of the detector in the peer-reviewed literature. The TK meter is a free-space coupled photoacoustic detector with an accurately known absorbance. The calibration of the TK meter is based

[4] The use of commercial names is for identification purposes only and does not constitute an endorsement by NIST.

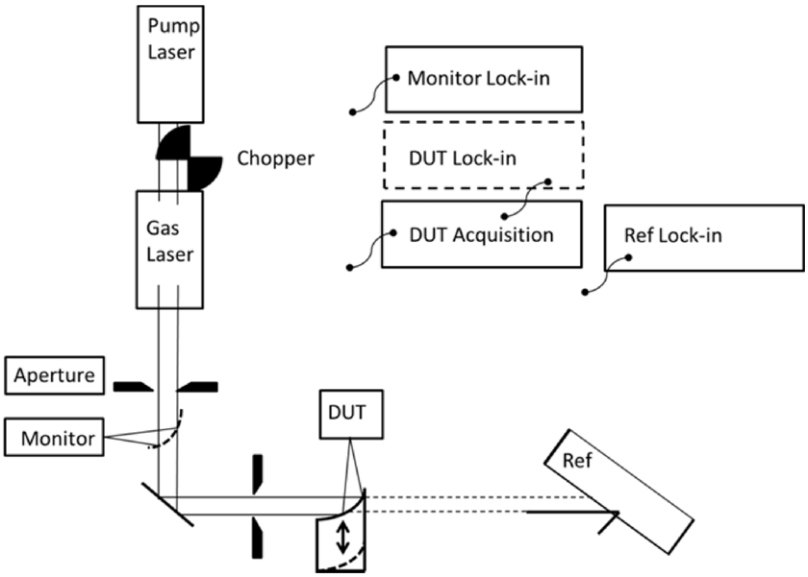

Figure 1. Schematic representation of the pyroelectric detector comparison. The primary beam is focused onto the pyroelectric DUT and collimated at the REF meter alternately. A portion of the primary beam is reflected from a dielectric beamsplitter (not shown) and focused onto the monitor detector.

on the electrical calibration (heating) of it, measured in current and resistance and expressed in watts. In every case, the commercially available meters were supplied with some means to express their output in terms of watts, but without being previously calibrated at 119 µm or 394 µm. Our measurement results are presented in terms of a calibration factor, C, the value of which should ideally approach unity.

The laser source consisted of a molecular gas laser pumped with a line-tunable carbon dioxide laser built at NIST. In the first instance, radiation of wavelength 119 µm was generated from methanol vapour, and in the second instance 394 µm was generated from formic-acid vapour. The laser beam had a nominal diameter of 10 mm.

Before the measurements began, the detector under test (DUT) was allowed to reach thermal equilibrium with the laboratory environment. Output from two of the pyroelectric detectors and two of the thermopiles was acquired by use of hardware and software provided by the manufacturer. In general, however, data from the pyroelectric detectors were recorded by use of a lock-in amplifier. Data from the thermopile detectors were acquired by means of a voltmeter. In each case, an optical chopper was placed between the pump laser and the molecular gas laser to reduce the contribution of background radiation. The measurement setup for the pyroelectric detectors and thermopile detectors is shown in figures 1 and 2, respectively. The pyroelectric detector evaluation is distinguished by use of an elliptical mirror having a gold coating (on a brass substrate). Polarization-dependent reflection losses attributable to this mirror were negligible. The description of the measurement and uncertainty follows.

3. Uncertainty contributions and data analysis

The uncertainty estimates for the NIST laser power and energy measurements are assessed following guidelines given by Taylor and Kuyatt [5]. To establish the uncertainty limits, the error sources are separated into (1) type B errors, whose magnitudes are determined by subjective judgment or other non-statistical method, and (2) type A errors, whose magnitudes are obtained statistically from a series of measurements. The expanded uncertainty was determined by combining the type A and type B 'standard uncertainties' in quadrature (the combined uncertainty) and multiplying this result by an expansion factor $k = 2$.

The responsivities of the detectors were evaluated by the method of direct substitution. The essential steps of this method are as follows. The laser power was simultaneously measured with the reference detector's response (REF) and the monitor detector's response (MON). The average ratio

$$\overline{S}_{\mathrm{REF}} = (\mathrm{REF}/\mathrm{MON})_{\mathrm{AVG}} \tag{1}$$

was calculated. Next, the DUT was substituted for the reference detector, and the laser power was simultaneously measured with response (DUT) and (MON). The ratio

$$\overline{S}_{\mathrm{DUT}} = (\mathrm{DUT}/\mathrm{MON})_{\mathrm{AVG}} \tag{2}$$

was calculated. Because of laser drift and other considerations the ratios in equations (1) and (2) were repeated multiple times. Therefore, for each detector we obtained a sequence ($i = 1, 2, 3, \ldots, n$) of measurement averages to determine n calibration factors:

$$C_i = 2(\overline{S}_{\mathrm{DUT}})_i/[(\overline{S}_{\mathrm{REF}})_i + (\overline{S}_{\mathrm{REF}})_{i+1}], \tag{3}$$

$$C_{i+1} = [(\overline{S}_{\mathrm{DUT}})_i + (\overline{S}_{\mathrm{DUT}})_{i+1}]/2(\overline{S}_{\mathrm{REF}})_{i+1}. \tag{4}$$

Three repeated episodes are illustrated in figure 3. The average and standard deviation of the set of factors $[C_1, C_2, C_3, \ldots, C_n]$ was then incorporated into the total uncertainty as a type A uncertainty, with $n = 12$.

The reference detector (TK meter) was evaluated with respect to variables that contribute to the measurement

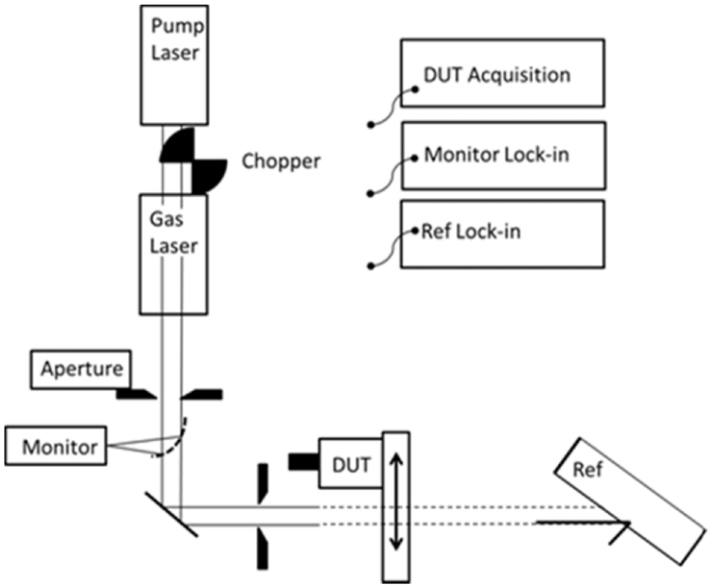

Figure 2. Schematic representation of the thermopile detector comparison. The DUT is translated in and out of the beam path during the measurement sequence.

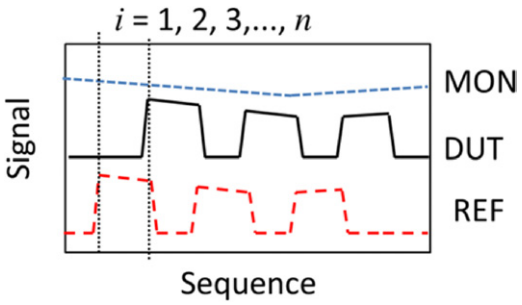

Figure 3. Graphical representation of a measurement episode.

uncertainty. The reference detector's absorbing element is a thin metallic film, whose surface impedance is close to half that of free space, deposited on a thin polymeric membrane (membrane thickness much less than one laser wavelength). Ideally, this configuration provides a frequency-independent absorbance of approximately 50%. In order to eliminate standing-wave effects from the polymethylpentene (TPX) windows (front and rear), the meter was oriented at Brewster's angle for the incident polarization (horizontal in these measurements). The reference detector's optical responsivity varies with chopping frequency f_c and optical frequency f_{THz} according to the following relationship:

$$R_{opt}(f_{THz}, f_c) = A R_{elec}(f_c)/T_{win}(f_{THz}), \tag{5}$$

where R_{elec} is the electrical responsivity, T_{win} is the transmittance of the TPX windows and A the film absorbance. R_{elec} was determined by electrical substitution as a function of frequency over the range 5 Hz to 100 Hz. The resistance of the meter's absorptive film was first measured, in four-terminal configuration, to be $R_{4T} = 162.73\,\Omega$ ($\pm 0.005\,\Omega$). A nominal 0 V to 5 V square wave was then applied to the film's 'probe' terminals (through a resistor), and a precision measurement of the electrical power made by measurements of the ac and dc voltages on a $6\frac{1}{2}$ digit multimeter. The equivalence between electrical and optical heating, particularly with respect to the area of electrical heating versus optical heating, has not been thoroughly evaluated. The quantity

$$\Delta P_e = R_{4T}^{-1}[(V_{dc} + V_{ac})^2 - (V_{dc} - V_{ac})^2] \tag{6}$$

represents the difference in electrical power levels; the nominal value for this difference was approximately 10.9 mW. For each frequency, the lock-in amplifier reading then provides the electrical responsivity,

$$R_{elec} = V_{lockin}/\Delta P_e. \tag{7}$$

All lock-in amplifier settings were identical to those used in the DUT measurements. The resulting electrical responsivity was analysed and empirically fitted to the sum of two single-pole roll-offs. The residuals to this fit yield a root-mean-square value of 0.04 V W^{-1}, or approximately 4%.

Transmittance of the TPX window was measured to account for losses due to scattering and absorptivity. Rather than disassemble the TK meter, two duplicate windows were obtained from Thomas Keating. The window transmittance was evaluated with a commercial FTIR instrument over a broad range of wavelengths spanning 119 µm and 394 µm. In addition, the transmittance was evaluated with the laser sources (119 µm and 394 µm) by comparing the TK-meter response with and without a separate window sample, at Brewster's angle, in the beam path. From the average of six laser measurements, the transmittance was determined to be 0.59 and 0.88 at 119 µm and 394 µm, respectively. The manufacturer specifies an uncertainty of the window transmittance of 2%. However, we adopt a more conservative uncertainty in order to account for the significant difference (as large as 5%) between our measured values and the manufacturer's specified value. A 5% type B value is assigned to this uncertainty based on the repeatability of the FTIR-based

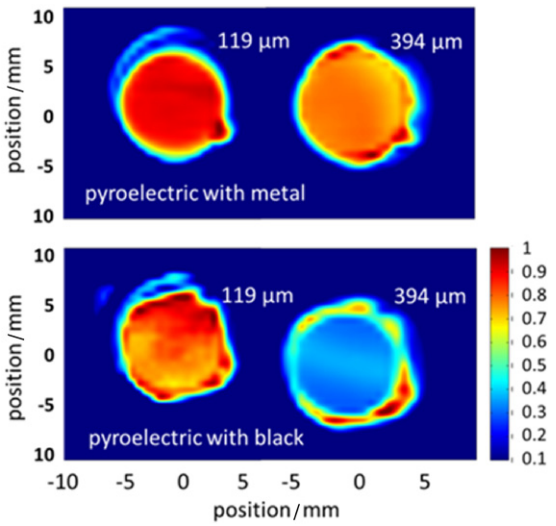

Figure 4. Relative spatial uniformity of the pyroelectric detectors at each wavelength.

measurements and the difference between our laser-based transmittance measurements and interpolated values obtained from the manufacturer.

The spatial uniformities of the pyroelectric detectors were evaluated at a power level of approximately 2 mW at the wavelengths 119 µm and 394 µm. In each instance, the laser beam was reflected and focused from a 13 mm aperture with a gold-coated, ellipsoidal mirror. The detector plane was located approximately at the focus, 20 mm from the mirror. In principle, based on calculation and knowledge of the mirror's f-number, greater than 99% of the total beam power was within a radius of 0.4 mm of the beam's centroid. The detector's response was obtained with a lock-in amplifier and by modulating the optical input at 25 Hz. The laser was moved across the detector's aperture at 0.6 mm intervals in a plane parallel to the detector plane with an automated positioning system composed of two orthogonal axes. The detector signal was sampled and recorded at each interval, and the data were normalized to the value of the highest response of any location on the detector. An example surface map of these data is shown in figure 4. The value of the spatial uniformity uncertainty is determined from a cross-section of the response variation. The spatial uniformity maps in figure 4 indicate a broad and uniform centroid with isolated peaks at the detector perimeter. The range of the uncertainty excludes the singularities of the perimeter and includes the central region spanning 5 mm in diameter. The spatial non-uniformity uncertainty is therefore a type B, with a value of 5% for the metal-coated pyroelectric detector and 2% for the detectors having a carbon-based coating.

The spatial uniformity of the thermopile detectors was not evaluated, because of the relatively long time constants of these detectors. It is possible to account for laser drift to accommodate the long time constant, but the laser would not operate continuously without having to purge, refill and realign the cavity. Because the nature of the carbon-based coatings on the thermopile is similar to that of the painted pyroelectric, we assigned a comparable type B uncertainty to these detectors. We consider this to be a conservative estimate because the laser beam area illuminated more than half of the active detector area (rather than being focused), and non-uniformities are substantially integrated. The non-uniformity of the thermopiles, however, has not been thoroughly evaluated.

Table 1. Summary of uncertainty contributions.

Variable	100 × Value
Electrical calibration	0.35
Lock-in gain	1.0
1/SNR	0.1
Spatial uniformity (reference)	1.0
Window transmittance	5
Film absorptance	2
Waveform mismatch	1.2
Laser amplitude drift	0.5 to 2.2
Path length	1.0
DUT electronics	0.35 to 1.0
DUT spatial uniformity	2 to 5
DUT C (type A)	0.5 to 13.4

In our method of direct substitution, there is a path-length difference for radiation travelling to the DUT compared to the reference. Therefore, some of the radiation is absorbed by the atmosphere, and the amounts of radiation reaching the individual detector surfaces are not equal. The amount of radiation absorbed over a 25 cm path length was calculated for 119 µm and 394 µm wavelengths, based on information available in the high-resolution transmission molecular absorption database (HITRAN) available from Harvard University (http://www.cfa.harvard.edu/hitran/). The absorption in air amounts to approximately 1%, which could be considered an offset. However, we were unable to confirm this number by direct measurement, and 1% is much smaller than the uncertainty of the relative absorptance. Therefore, we assign a type B uncertainty of 1% to acknowledge this contribution.

The contribution of uncertainty from electronic instrumentation used in this measurement is relatively small. A conservative estimate is presented by merely using the values provided by the manufacturer. This is typically treated as a type B uncertainty. The main components of concern, not accounted for in the reference detector evaluation, are the voltmeter used with the thermopiles and the lock-in used for the pyroelectric detectors. For these instruments, we use values of 0.35% and 0.1%, respectively.

Variation in the pointing stability of the laser was considered with respect to the monitor beam input. Radiation is focused onto the monitor detector by means of an off-axis paraboloid. The focused beam is less than one tenth the size of the detector. An approximation of the required pointing variation requires a variation greater than 4°, and in the worst case, would be extremely difficult to isolate from the inherent laser amplitude drift. Thus, we consider the pointing instability to be negligible and no uncertainty value is included.

A value of the laser amplitude drift during the measurement is captured in the monitor detector's output. Laser amplitude drift is corrected for through use of the monitor detector (see figure 1). However, this correction has an uncertainty associated with it, and this uncertainty is larger

Table 2. Summary of measurement results and uncertainties.

Detector description, coating (diameter)	C at 119 µm	$100 \times U(k = 2)$	C at 394 µm	$100 \times U(k = 2)$
Pyroelectric detector, metal (∅10 mm)	0.1371	7.50	0.1568	7.12
Pyroelectric detector, organic black (∅10 mm)	0.5609	11.94	0.1698	7.92
Thermopile, organic black (∅10 mm)	0.5625	9.10	0.4381	8.46
Thermopile, high damage threshold black (∅10 mm)	0.4880	9.04	0.0704	7.36
Thermopile, organic black (∅25 mm)	0.5537	13.94	0.4376	9.22
Thermopile, organic black (∅25 mm)	0.7637	9.72	0.3752	10.74
Thermopile, VANTA (∅25 mm)	0.9476	14.66	0.9618	9.7

for the thermopile detectors that have a longer time constant and thus a longer measurement period. This drift is assigned a type B uncertainty and differs for each detector. The largest drift value was 2.2% for one period in the sequence depicted in figure 3.

The uncertainty contributions are summarized in table 1. The calibration factors and the expanded relative uncertainty calculated with values presented in table 1 are in table 2.

Nominally, the units of each calibration factor, C, are W/W, that is, power measured by the DUT divided by power measured by the reference detector. With the exception of the VANTA thermopile, the magnitude of the responsivity of the DUT is based on its previous calibration at either 1.064 µm or 10.6 µm, where such calibrations are commonly available. The fact that the calibration factors are significantly below unity emphasizes the need for FIR laser power-meter calibrations. It is fair to say that the results for the commercial detectors are not based on an inaccurate previous calibration, but simply on a different calibration that is inappropriate for this comparison. We attribute the low calibration factors substantially to reflectance losses from the DUT coating in the FIR. Furthermore, with the exception of the metal-coated pyroelectric and the VANTA thermopile, the responsivity is not spectrally uniform from 119 µm to 394 µm.

4. Conclusion

We have described the method of direct substitution to evaluate the responsivity of several commercially available thermal detectors, in addition to a novel thermopile having a carbon nanotube array. The detector responsivity measurement results, as well as the uncertainty of the measurement, demonstrate that the nanotube-coated detector has a relatively higher and spectrally uniform response compared to a similar thermopile coated with carbon-based paint. The responsivity at 394 µm of those detectors coated with black paint was significantly lower than the responsivity at 119 µm. The responsivity of the chromium-coated pyroelectric detector, however, was similar at each wavelength as expected. For metrological purposes, the extent to which the coating absorbance is spectrally uniform and quantifiable is as important as high efficiency. The characterization of absorber coatings for far-infrared and terahertz detectors bears further investigation. In particular, complete scattering parameters of vertically aligned carbon nanotube arrays as a function of tube length are needed.

Acknowledgment

The authors thank Malcolm White for helpful discussions regarding the data analysis.

References

[1] Popovic Z and Grossman E N 2011 THz metrology and instrumentation *IEEE Trans. Terahertz Sci. Technol.* **1** 133–44

[2] Dietlein C, Popovic Z and Grossman E N 2008 Aqueous blackbody calibration source for millimeter-wave/terahertz metrology *Appl. Opt.* **47** 5604–15

[3] Steiger A, Gutschwager B, Kehrt M, Monte C, Müller R and Hollandt J 2010 Optical methods for power measurement of terahertz radiation *Opt. Express* **18** 21804–14

[4] Lehman J H, Lee B and Grossman E N 2011 Far infrared thermal detectors for laser radiometry using a carbon nanotube array *Appl. Opt.* **50** 4099–104

[5] Taylor B N and Kuyatt C E 1994 *NIST Technical Note 1297, 'Guidelines for Evaluating and Expressing the Uncertainty of NIST Measurement Results'* (National Institute of Standards and Technology) 20 pp